Carbohydrate Polymers 115 (2015) 348–355

Contents lists available at ScienceDirect

Carbohydrate Polymers

journal homepage: www.elsevier.com/locate/carbpol

Electrospinning of agar/PVA aqueous solutions and its relation with rheological properties

Ana M.M. Sousa[a,b], Hiléia K.S. Souza[a], Joseph Uknalis[b], Shih-Chuan Liu[b,c], Maria P. Gonçalves[a], LinShu Liu[b,*]

[a] REQUIMTE, Faculdade de Engenharia, Universidade do Porto, Rua Dr. Roberto Frias, 4200-465 Porto, Portugal
[b] Eastern Regional Research Center, Agricultural Research Service, United States Department of Agriculture, 600 East Mermaid Lane, Wyndmoor, PA 19038, USA
[c] School of Health Diet and Industry Management, Chung Shan Medical University and Department of Nutrition, Chung Shan Medical University Hospital, 110, Section 1, Jian-Guo North Road, Taichung 402, Taiwan, ROC

ARTICLE INFO

Article history:
Received 10 June 2014
Received in revised form 8 August 2014
Accepted 10 August 2014
Available online 2 September 2014

Keywords:
Agar
PVA
Electrospinning
Tubeless spinneret
Rheology
Nanofibers

ABSTRACT

In this work, we report the successful fabrication of agar-based nanofibers by electrospinning technique, using water as solvent media. A tubeless spinneret was attached inside the electrospinning chamber, operating at 50 °C, to avoid agar gelation. Agar pure solution (1 wt%) showed inadequate spinnability regardless of the used electrospinning conditions. The addition of a co-blending polymer such as PVA (10 wt% starting solution) improved the solutions viscoelasticity and hence, the solutions spinnability. Agar/PVA solutions were prepared with different mass ratios (100/0, 50/50, 40/60, 30/70, 20/80 and 0/100) and electrospun at various sets of electrospinning conditions. Best nanofibers were obtained with 30/70 and 20/80 agar/PVA blends while samples with higher agar contents (50/50 and 40/60 agar/PVA) were harder to process and led to discontinuous fibrous mats. This first set of encouraging results can open a new window of opportunities for agar-based biomaterials in the form of nanofibers.

Published by Elsevier Ltd.

1. Introduction

Nanofibers are exciting forms of biomaterials used for the transport and release of targeted compounds, tissue engineering, surface modification of implants, enzyme mobilization, wound dressing, and others (Agarwal, Wendorff, & Greiner, 2008; de Moraes & Beppu, 2013; Luo, Wang, et al., 2013; Ma, Fang, Liu, Zhu, & Nie, 2012; Toskas et al., 2011). The use of natural polymers such as chitosan, cellulose or alginate to fabricate nanofibers for biomedical applications, is seen with particular interest since their degradation products can be incorporated into normal metabolic pathways of the host, avoiding potential side effects (Bonino et al., 2011; Jayakumar, Menon, Manzoor, Nair, & Tamura, 2010; Luo, Wang, et al., 2013; Schiffman & Schauer, 2008). At the same time, natural polymers typically present excellent cell adhesion, proliferation and differentiation (Krishnan, Sundarrajan, & Ramakrishna, 2013). In the particular case of seaweed polysaccharides, the preference for alginate relies on its ability to form insoluble polymeric structures in the presence of divalent ions (Rinaudo, 2008). More recently, polysaccharides from the green seaweed *Ulva* have also shown potential for fiber formation when blended with polyvinyl alcohol (PVA) (Toskas et al., 2011). PVA is a cheap, water soluble, non-toxic and biocompatible polymer, many times used in biomedical applications (Greiner & Wendorff, 2007; Hassan & Peppas, 2000). For these reasons, and due to its excellent spinnability, PVA is frequently considered as co-blending polymer in electrospinning processes (Greiner & Wendorff, 2007).

Agar is a complex mixture of gelling polysaccharides found in selected marine red seaweeds. It is build up on agarose, the unbranched gelling segment of the polymer skeleton, *i.e.* 3-linked β-D-galactose (G) and 4-linked 3,6-anhydro-α-L-galactose (LA) units, and agaropectin, formed by G, LA and 4-linked α-L-galactose (L) residues masked by the presence of several substituent groups (*e.g.* sulfate esters, methyl ethers, pyruvate acid ketals) (Matsuhashi, 1990). Unlike alginate or ulvan, agar does not require additives (such as salts) to form gels which makes it more challenging to process in other forms besides gels (Khanarian, Haney, Burga, & Lu, 2012; Rodrigues et al., 2012; Santoro et al., 2011; Yamada et al., 2012). The use of agar nanofibers could potentiate new and exciting properties of the polymer, not seen at greater scales (Greiner & Wendorff, 2007).

---

* Corresponding author. Tel.: +1 215 233 6486.
E-mail address: LinShu.liu@ars.usda.gov (L. Liu).

http://dx.doi.org/10.1016/j.carbpol.2014.08.074
0144-8617/Published by Elsevier Ltd.

Electrospinning is one of the most popular methods for preparing fibers at nano-scale (Greiner & Wendorff, 2007; Luo, Stoyanov, Stride, Pelan, & Edirisinghe, 2012; Schiffman & Schauer, 2008). Basically, high voltage is applied to the polymer solution or melt, held at a tip of a capillary by its surface tension. When the applied electric field overcomes the surface tension of the droplet, a jet travels toward the grounded collector with opposite charge, placed at a known distance from the needle tip. If volatile solvents are used (*e.g.* water), the solvent will evaporate as the jet travels toward the counter electrode. The feed rate of the solution, the applied electric field, the distance tip-to-collector or the environmental conditions (temperature and relative humidity) must be carefully controlled, in order to obtain adequate fibers. Other fundamental parameters related with the solution (*e.g.* concentration, viscosity, viscoelasticity, electric conductivity, surface tension) and naturally, the polymer and solvent intrinsic properties (*e.g.* melting point, molecular weight, entanglement density) will be determinant for fiber formation (Greiner & Wendorff, 2007).

In this work, we report our attempts of producing agar nanofibers by electrospinning technique. To the best of our knowledge, the successful application of electrospinning to agar aqueous solutions has not yet been reported. Only one paper was found describing the fabrication of agar and agarose fibers through wet-spinning using dimethyl sulfoxide (DMSO) aqueous media. The formed materials presented fiber diameters in the range 74–123 μm (Bao, Hayashi, Li, Teramoto, & Abe, 2010). In our case, to overcome agar processing difficulties due to gelation, a tubeless spinneret was placed inside the electrospinning chamber, operating at 50 °C. To improve agar's spinnability, PVA was used as a co-blending polymer. The rheological behavior of the spinning solutions, prepared at different mass ratios (100/0, 50/50, 40/60, 30/70, 20/80 and 0/100 agar/PVA) from starting solutions of agar and PVA with, respectively, 1 wt% and 10 wt%, was analyzed through dynamic oscillatory and steady shear tests. The morphology of the nanofibers obtained at different electrospinning conditions was investigated by SEM and correlated with the rheological properties.

2. Materials and methods

2.1. Chemicals

Commercial agar (A-7002, St. Louis, MO, $(C_{12}H_{18}O_9)_n$) and PVA (average M_w = 89,000–98,000 Da, 99+% hydrolyzed; $(CH_2CHOH)_n$) were purchased from Sigma–Aldrich Co. Relevant physicochemical properties of the agar sample (LA ~ 43.5% and sulfate ~ 1.6% contents; intrinsic viscosity, $[\eta] \sim 3.5$ dL/g; viscosimetric molecular mass, $M_v \sim 138$ kDa; gel strength, GS ~ 1177 g cm^{-2} for a 1.5 wt% agar solution) were determined previously by our group, following standard procedures (Sousa, Borges, Silva, & Gonçalves, 2013; Sousa, Borges, Silva, Ramos, et al., 2013).

2.2. Preparation of agar/PVA spinning solutions

Agar and PVA powders were pre-dried overnight at 40 °C in a vacuum oven, prior to use. Each starting solution was prepared by dissolving the appropriate amount of polymer in water, as described next.

The concentrations of the starting solutions were 1 wt% for agar and 10 wt% for PVA. This choice was based on preliminary tests and considering the intrinsic properties of each polymer. The agar powder was dispersed in cold water and dissolved at temperatures close to the boiling point of the solvent, under vigorous stirring. Special caution was taken when dissolving PVA; to avoid the formation of lumps and/or a PVA film at the solution surface, a heating bath and stirrer promoting an evenly dispersion of all PVA particles were used. The PVA powder was dispersed in water and dissolved at ~90 °C, under mild mixing conditions. Both polymers were considered dissolved when a homogeneous transparent solution was obtained.

Agar/PVA blends with different mass ratios (*i.e.* 100/0, 50/50, 40/60, 30/70, 20/80, 0/100) were prepared by weighing the appropriate amounts of each starting solution into closed cap vials. Finally, the mixtures were heated again close to the solvent's boiling point (~94 °C), under vigorous stirring, until a homogeneous solution was obtained. In each case, the samples were degassed in a vacuum oven for 5 min at 90 °C and, to prevent gelation, kept at temperatures above 50 °C, until the rheological and electrospinning experiments were carried out.

2.3. Rheological characterization of the spinning solutions

The rheological measurements used to characterize the spinning solutions were performed in a stress-controlled rheometer (ARG2, TA Instruments, USA). A cone-and-plate geometry (4 cm diameter, 2° angle and a 54 μm gap) was used in all cases. The samples were loaded while hot into the measuring device, pre-heated at 90 °C. Each sample was covered with a layer of paraffin oil to prevent water evaporation during the course of the experiments. Samples were cooled down from 90 to 50 °C at a cooling rate of 1 °C/min and a fixed frequency of 6.28 rad/s. After an equilibration period at 50 °C, frequency scans were recorded over the range 1–75 rad/s. The strain conditions were chosen according to the linear viscoelastic region defined during strain sweep tests. A common strain of 1% was selected for the several aqueous media. Steady shear measurements were also carried out at 50 °C, the chosen temperature for the electrospinning experiments (*i.e.* 50 °C), in the range 1–200 s^{-1}. The shear rate was recorded point by point with a maximum point time of 1 min. The curves were built from viscosity data determined for each point as an average of three consecutive measurements with a maximum 5% deviation. Three replicates were performed in each case.

2.4. Fabrication of agar/PVA fibers by electrospinning technique

Processing polysaccharide solutions in electrospinning is quite challenging due to the long-range electrostatic interactions as well as the presence of counter ions experienced by these compounds (Schiffman & Schauer, 2008). In the specific case of seaweed polysaccharides, the electrospinning achievements so far seem rather modest, most likely due to the complex nature of both, compounds and process. Pure solutions of seaweed polysaccharides seem inadequate for electrospinning (Stijnman, Bodnar, & Tromp, 2011) much due to the repulsive forces existent in the polyelectrolyte solutions (Schiffman & Schauer, 2008). To overcome this limitation, co-bending polymers such as PEO and PVA (Lu, Zhu, Guo, Hu, & Yu, 2006; Safi, Morshed, Ravandi, & Ghiaci, 2007) and/or strong polar cosolvents such as glycerol (Nie et al., 2008) have been added with success to alginate solutions to produce nanofibers. Also, Toskas et al. (2011) manage to fabricate ulvan nanofibers using as solvent a mixture of H_3BO_3 and $CaCl_2$ aqueous solutions and PVA as carrier polymer. The challenge with electrospinning agar would be even greater due to its exquisite gelling capability. For that reason, we propose a different approach to electrospin aqueous solutions of agar, described in detail next. The electrospinning unit used to carry out the experiments was from NaBond Technologies Co., Ltd., China. A schematic representation of the equipment is given in Fig. 1. To overcome the processing difficulties due to agar's gelling nature at room temperature, a tubeless spinneret (NaBond Technologies Co., Ltd., China) was attached inside the chamber and connected to the external syringe pump (Veryark, model TCI-IV).

This accessory requires a minimum solution volume for each experiment (0.5 mL) and no soft tube is needed for connecting the needle to the syringe. This allows the syringe with the polymer solution to be placed inside the chamber at the temperature defined for the test. In our case, 50 °C was the chosen temperature to carry out the experiments (maximum working temperature of the equipment). The connection between the syringe pump and the tubeless spinneret was accomplished by a soft plastic tube containing water. The flow rate set on the syringe pump forced the piston of the syringe carrying the solution to move. In all cases, the samples were placed in a 5 mL plastic syringe fitted with a metallic needle (outer diameter × length = 0.6 mm × 30 mm and inner diameter = 0.317 mm). A high voltage power supply device (0–50 kV) was used to generate the high electric fields. For each solution, several operational conditions were tested including flow rate (0.5–16 mL/h), voltages (10–30 kV) and distance tip-to-collector (6–12 cm). After several trials, the distance tip-to-collector was fixed at 8 cm. A drum collector covered with an aluminum foil was chosen to collect the electrospun materials. The spinneret was fixed (null *x*-axial sliding) and the motor speed of the collector was around 510 rps in all cases.

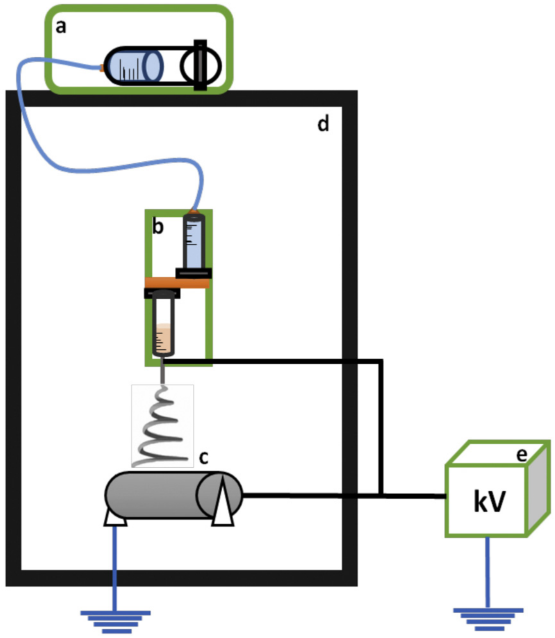

Fig. 1. Schematic representation of the electrospinning setup used to fabricate agar/PVA nanofibers (a – syringe pump; b – tubeless spinneret; c – drum collector; d – chamber with temperature control; e – power supply).

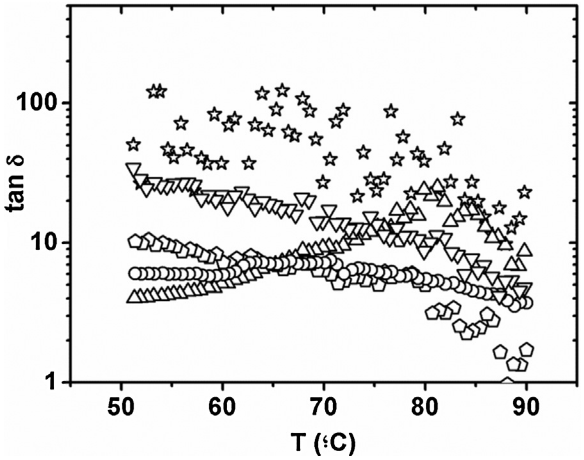

Fig. 2. Temperature dependence of tan δ of agar/PVA aqueous mixtures (0/100 (inverted triangles), 20/80 (circles), 30/70 (triangles), 40/60 (pentagons) and 50/50 (stars) mass ratios), during a cooling ramp from 90 to 50 °C, recorded at 6.28 rad/s and 1% strain amplitude. The blends were prepared from a 1 wt% agar and 10 wt% PVA starting solutions.

2.5. Scanning electron microscopy (SEM)

The morphology and size of the fibers were investigated by scanning electron microscopy in a Quanta 200 FEG scanning electron microscope (SEM, FEI, Hillsboro, OR). Each sample was mounted with adhesive to specimen stubs, and the edge painted with colloidal silver adhesive. Afterwards, it was coated with thin film of gold and imaged in the high-vacuum/secondary electron imaging mode SEM using an accelerating voltage of 10 kV and working distances around 10 mm.

3. Results and discussion

3.1. Rheological characterization of the spinning solutions

The rheological behavior of the spinning solutions prepared at different agar/PVA mass ratios was analyzed through dynamic oscillatory and steady-shear tests.

At 50 °C, the pure agar solution (1 wt%) showed extremely low values of G' and G'' as well as apparent viscosity, η_{app} (~0.015 Pa s) over the course of the rheological experiments. For this reason and due to the significant scattering of the viscoelastic data, no curves will be presented for this sample.

Data from the cooling ramps performed from 90 to 50 °C (Fig. 2), indicated predominance of the viscous component ($G'' > G'$ or tan $\delta > 1$) for all samples. This behavior, typical of macromolecular solutions, was expected since we were above the temperature range defined for agar's gelation, ~30–40 °C (Matsuhashi, 1990). According to the proposed model for agar gelation (Djabourov, Clark, Rowlands, & Ross-Murphy, 1989), this temperature window should match a random coil state for agar molecules. In aqueous media, agar molecules are believed to suffer a transition from a disordered state (*i.e.* random coil) to an ordered conformation (double helices formation followed by intensive interhelical association) when cooled to temperatures below the polymer's gelation point (Djabourov et al., 1989; Sousa, Borges, Silva, & Gonçalves, 2013; Sousa, Borges, Silva, Ramos, et al., 2013). PVA in turn, typically needs to be crosslinked by crosslinking agents, chemical crosslinking or freeze–thawing methods (*i.e.* 'physical crosslinking) to develop a gel structure (Hassan & Peppas, 2000). The large number of hydroxyl groups throughout PVA's backbone forms strong intra- and intermolecular hydrogen bonding that will shape its bulk properties (Gao, Yang, He, & Yang, 2010). This will be more significant for PVA with higher hydrolysis degree (*i.e.* more hydroxyl groups) which will need to be heated at higher temperatures (typically above 80 °C) to be dissolved in water. The heat causes the disruption of the intra- and intermolecular hydrogen bonds and the solubility of the polymer in aqueous media is increased. During the process, new hydrogen bonds are formed between PVA and water while part of the inter- and intra-chain PVA bonds remain. Upon cooling, the disrupted bonds can be formed again, leading to an increase in viscosity (Briscoe, Luckham, & Zhu, 2000; Koski, Yim, & Shivkumar, 2004).

The addition of PVA to agar, led to solutions with different elasticities (Fig. 2). 50/50 agar/PVA, with higher agar amount, exhibited greater data scattering (probably close to the detection limit of the equipment). When higher amounts of co-blending polymer were added (40/60, 30/70 and 20/80 agar/PVA), the systems seemed to gain elasticity when compared to the pure PVA solution. However,

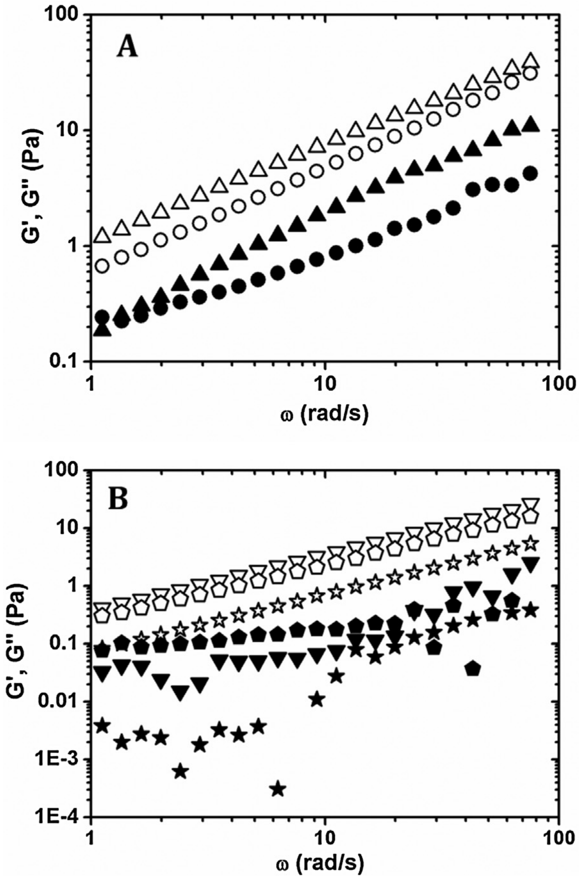

Fig. 3. Frequency dependence at 50 °C of elastic (G'; filled symbols) and viscous (G''; open symbols) moduli of agar/PVA aqueous blends ((A): 30/70 (triangles) and 20/80 (circles) mass ratios; and (B): 40/60 (pentagon), 50/50 (stars) and 0/100 (inverted triangles) mass ratios), recorded at 6.28 rad/s and 1% strain amplitude. The blends were prepared from a 1 wt% agar and 10 wt% PVA starting solutions.

a higher precision rheometer would be needed to decrease the data scattering and further confirm this trend.

The equilibration step of agar/PVA blends recorded at 50 °C, confirmed the predominance of the viscous component (*i.e.* $G'' > G'$; not shown). In all cases, the viscoelasticity of the systems was not undergoing appreciable changes that could compromise acquiring the mechanical spectra. At 50 °C, the mechanical spectra, showed $G'' > G'$ over the entire range of considered ω, for all agar/PVA blends, which is typical of macromolecular solutions (Fig. 3). Here, as well, the elastic component of the blends with higher agar contents (*e.g.* 50/50 and 40/60 agar/PVA; Fig. 3B) showed some data dispersion which was attributed to the low concentration of the samples. The 30/70 and 20/80 agar/PVA blends described close viscoelastic curves (Fig. 3A).

According to Rošic et al., rheological parameters in bulk (those studied in the present work) and at the interface are important for predicting the electrospinnability of polymer solutions and have to be taken as complementary. Bulk properties are largely determined by polymer concentration and thus directly affect jet initiation, while the interfacial properties determine the continuation of the jet and fiber formation (Rošic et al., 2012). In their study, the interfacial measurements showed the same parameter trends as was observed in the bulk. However, the values of the interfacial rheological parameters were three orders of magnitude lower than those observed in the bulk.

Overall, the systems exhibited weak shear thinning behavior characterized by a decrease in viscosity upon increase of shear rate when relevant shear forces were applied (Fig. 4). This behavior seemed to be attenuated with the increase of agar content, and consequent PVA decrease, in the final blend (*e.g.* 50/50 agar/PVA). Shear thinning systems are characterized by the disruption of some intermolecular entanglements and simultaneously the formation of new ones enabling the viscosity of the system to stay approximately constant, in the region of low shear rates. When a shear rate threshold is attained, the system disturbance becomes too significant and the formation of new entanglements no longer compensates the intermolecular disruptions. At this point, the molecular alignment in the flow direction takes place causing the viscosity of the system to decrease (Bastos et al., 2010). The deviations observed in the region of low shear rates might be explained by the limited number of inter-chain hydrogen bonds leading to thinning due to the bonds breaking under low shears (Gao et al., 2010). Zadeh, Keyanpour-Rad, and Ebadzadeh (2014) found that while PVA solutions with low concentration (<5%) exhibited Newtonian behavior, higher PVA contents (6–10%) showed shear thinning behavior. Similar non-Newtonian behaviors were reported by Toskas et al. (2011) when using PVA as co-blending polymer in related polysaccharide systems.

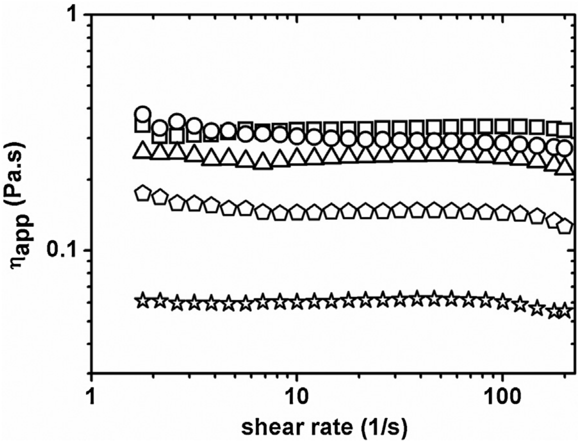

Fig. 4. Representative curves of the shear-dependence of the apparent viscosity of agar/PVA aqueous blends (0/100 (squares), 20/80 (circles), 30/70 (triangles), 40/60 (pentagons) and 50/50 (stars) mass ratios) at 50 °C. The blends were prepared from a 1 wt% agar and 10 wt% PVA starting solutions.

Around 10 s^{-1} (deformation rate felt in the needle; Stijnman et al., 2011), the solutions exhibited increasing viscosities with the increase of PVA concentration in the final blend: η_{app} were ~0.32, ~0.30, ~0.24, ~0.15, ~0.06 Pa s for respectively, 0/100, 20/80, 30/70, 40/60 and 50/50 agar/PVA. In the range of deformation rates felt in the Taylor cone and jet (800–1200 s^{-1}; Han, Yarin, & Reneker, 2008) however, it was hard to obtain reproducible data (not shown). Hence, the flow properties were measured in a narrower range of shear rates.

The Cox Merz rule (Eq. (1)), used to correlate the properties measured in the regime of small and linear deformations (dynamic oscillatory studies) and the properties in the regime of large and non-linear deformations (steady shear tests), was applied to the experimental data. This rule establishes the superposition of the shear rate dependence of the steady shear viscosity, $\eta(\dot{\gamma})$, with the frequency dependence of the magnitude of the complex viscosity, $|\eta^*|(\omega)$, at equal values of ω and $\dot{\gamma}$,

$$|\eta^*|(\omega) = \eta(\dot{\gamma})\Big|_{\omega=\dot{\gamma}} \tag{1}$$

Deviations from this empirical rule may be indicative of the formation of a weakly structured material and consequently, solutions with poorer spinnability. As examples, the combined plots of Cox Merz rule for 0/100 and 40/60 agar/PVA blends are given in Fig. 5, while the 20/80 system is shown as inset graph. Remaining

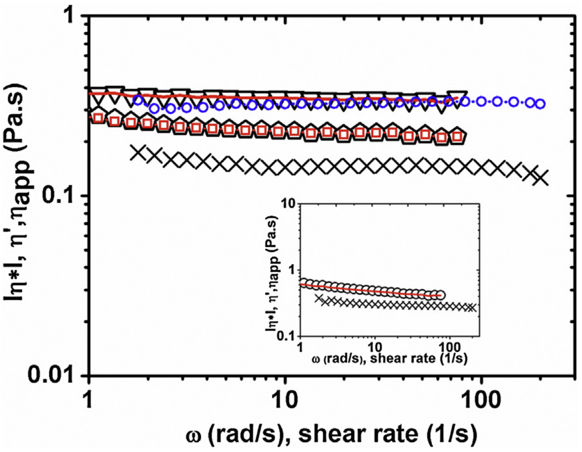

Fig. 5. Combined plot of the magnitude of complex viscosity, $|\eta^*|(\omega)$ (main graphic: open inverted triangles, open pentagons; inset: open circles), dynamic viscosity, $\eta'(\omega)$ (main graphic: red line, red open squares; inset: red line) and apparent viscosity, $\eta(\dot{\gamma})$ (main graphic: blue line with open circles, crosses; inset: crosses) at 55 °C, according to the Cox–Merz rule, for respectively, 0/100 and 40/60 agar/PVA (main graphic) and 20/80 agar/PVA (inset) solutions. (For interpretation of the references to color in this figure legend, the reader is referred to the web version of this article.)

systems described similar trends (not shown). While dynamic and steady shear data from pure PVA obeyed the principle of superposition, agar/PVA blends showed deviations from Cox Merz rule. These departures could be attributed to structure decay due to the effect of the strain deformation applied to the system, which is low in oscillatory shear, but is high enough in steady shear to break down structured intermolecular associations. In this case, the complex viscosity is usually higher than the steady viscosity (Sittikijyothin, Sampaio, & Gonçalves, 2010).

3.2. Electrospinning

The detailed operational conditions at which the fibers were obtained as well as relevant observations concerning the experiments are listed in Table 1. Some operational parameters were fixed and chosen based on preliminary trials. For instance, the distance tip-to-collector (8 cm) was such that guaranteed the stability and direction of the polymer jet toward the counter electrode. The sample volume was 3 mL while the needle size was the lowest possible available (inner diameter = 0.317 mm). Other parameters such as working temperature and concentration of the starting polymer solutions were defined according to the physicochemical properties of the polymers. To avoid as much as possible agar gelation during the experiments, the electrospinning chamber was set at the maximum possible working T (*i.e.* 50 °C). In addition, a tubeless spinneret was placed inside the chamber and connected to a syringe pump placed outside the chamber using a soft plastic tube in order to keep the spinning solution warm during the process (Fig. 1).

Agar pure solution (1 wt%) was impossible to be successfully spun at any set of electrospinning parameters. Droplets fell down from the needle tip in all cases revealing inadequate viscoelasticity of the solution (Nie et al., 2008). Rheological data confirmed this interpretation. Even though low polymer concentration can hinder nanofibers formation due to insufficient chain entanglements (Toskas et al., 2011), higher concentrations would lead to agar gelation and consequently, obstruction of the needle.

In order to improve agar spinnability, PVA was added to the pure polysaccharide medium. PVA is a semi-crystalline and water soluble polymer extensively used for the fabrication of nanofibers due to its good biocompatibility, non-toxicity and excellent spinnability (Koski et al., 2004; Rošic et al., 2012; Toskas et al., 2011). A starting solution of 10 wt% PVA concentration was considered adequate to obtain agar/PVA blends with satisfactory spinnability. While insufficient PVA concentration would lead to electrospraying of the spinning solution, excess of PVA content could result in bead formation (Santos et al., 2014). Micrographs of the agar/PVA fibers prepared at various processing conditions and agar/PVA mass ratios, are represented in Fig. 6. For each composition, the operational parameters summarized in Table 1 were chosen based on the best possible polymer jet (*i.e.* uniform spinning or ejection).

Blends with higher agar contents (40/60 or 50/50 agar/PVA) were harder to process. At these ratios, the needle would be obstructed in the early stage of the spinning process and the experiment stopped. Considering that the spinning solution was placed inside the chamber at temperatures well above 50 °C and that at this temperature the systems exhibited typical behavior of entangled polymer solutions (Fig. 3), this indicated that the solutions were actually being spun at temperatures below 50 °C. Even if the temperature controller provided by the manufacturer could lack some accuracy, the draconian conditions that this kind of processes imply, makes it difficult a stricter control of the environment conditions. In most of the cases, shower jets intercalated with droplets were observed. The droplets persisted even after mixing both polymers under heat for a significant time-frame which could indicate limited compatibility between agar and PVA in aqueous media. That is, PVA full of hydroxyl groups might establish limited intermolecular associations with agar through hydrogen bonding due to a greater propensity to re-form intra chains entanglements upon cooling as the jet travels to the collector or during solvent evaporation (Koski et al., 2004). Based on the jets of the pure polymer solutions, the droplets were attributed to agar rich-phase regions on the spun solution.

Tests of the 50/50 agar/PVA blend were carried out between 14 and 24 kV, range at which a polymer jet of any kind was pulled out from the needle. The ejected solutions were more uniform at low flow rates hence the material was collected at 0.7 mL/h (E.1 conditions in Table 1). Discontinuous fibrous mats were observed for 50/50 and 40/60 agar/PVA blends (Fig. 6A and B) which might indicate insufficient entanglement density (*i.e.* low concentration) or excess voltage causing inadequate instabilities during the jet formation (Barber, Griggs, Bonner, & Rogers, 2013; Bonino et al., 2011). The frequency scans and flow curves recorded for these samples seemed to agree well with this view (Figs. 3B and 4). The irregularity in shape was significant, with fibers and beaded fibers of variable diameters being formed. For the 40/60 blend, higher flow rates were the most adequate (E.2 conditions in Table 1).

When increasing the PVA concentration in the final mixture, the morphology of the collected fibers was significantly improved (*i.e.* 30/70, 20/80 and 0/100 agar/PVA blends; Fig. 6C–F). This matched an increase in apparent viscosity measured through the steady state shear tests (Fig. 4) due to a greater influence of PVA to the systems' behavior. Individual nanofibers were seen in majority although some fiber doublets or partially fused fibers as well as fibers exhibiting branching could be seldom identified (Fig. 6D; Peresin et al., 2010). Some of the fibers seemed also flattened which could have been caused by the higher viscosity and solution concentration causing the solvent evaporation to occur more slowly and the wet fibers that reached the drum collector to be flattened by the impact (Zadeh et al., 2014). A close inspection of Table 1 and Fig. 6D and E point out to the effectiveness of high flow rates and voltages in preventing the formation of beaded fibers at 20/80 agar/PVA ratio (E.4 *vs* E.5 conditions). Of particular interest were the E.4 conditions (14 mL/h and 24 kV) where the homogeneity of the obtained fibrous mat was quite evident (Fig. 7A). When the flow rate was lowered to 6 mL/h (E.5 conditions) and the voltage set at its maximum (30 kV), some beads could be rarely detected (Fig. 7B). It is worth noting that,

Table 1
Details of the electrospinning experiments concerning the fabrication of agar/PVA nanofibers. The following conditions were fixed in all experiments: temperature of 50 °C, initial sample volume of 3 mL and distance tip-to-collector of 8 cm. A drum collector was used in all cases. For more details concerning the overall process please see Section 2.

Conditions Id	Figure Id	Agar conc. (wt%)	PVA conc. (wt%)	Agar/PVA ratio	Volume (mL)	Flow rate (mL/h)	Voltage (kV)
E.1	6A	1	10	50/50[a]	3	0.7	24
E.2	6B	1	10	40/60[a]	3	6	20
E.3	6C	1	10	30/70	3	14	24
E.4	6D/7A	1	10	20/80	3	14	24
E.5	6E/7B	1	10	20/80	3	6	30
E.6	6F	1	10	0/100	3	14	24

[a] At some point the needle was obstructed due to agar gelation.

at this lower flow rate, a 24 kV voltage was ineffective at producing consistent nanofibers.

Agar gelation occurs gradually, the viscoelastic transition happening over a broad temperature window, ~43–30 °C (Sousa, Borges, Silva, & Gonçalves, 2013; Sousa, Borges, Silva, Ramos, et al., 2013). Even though the equipment was setup to operate at 50 °C, for longer processing times the samples would approach the region of significant viscoelastic transitions causing the obstruction of

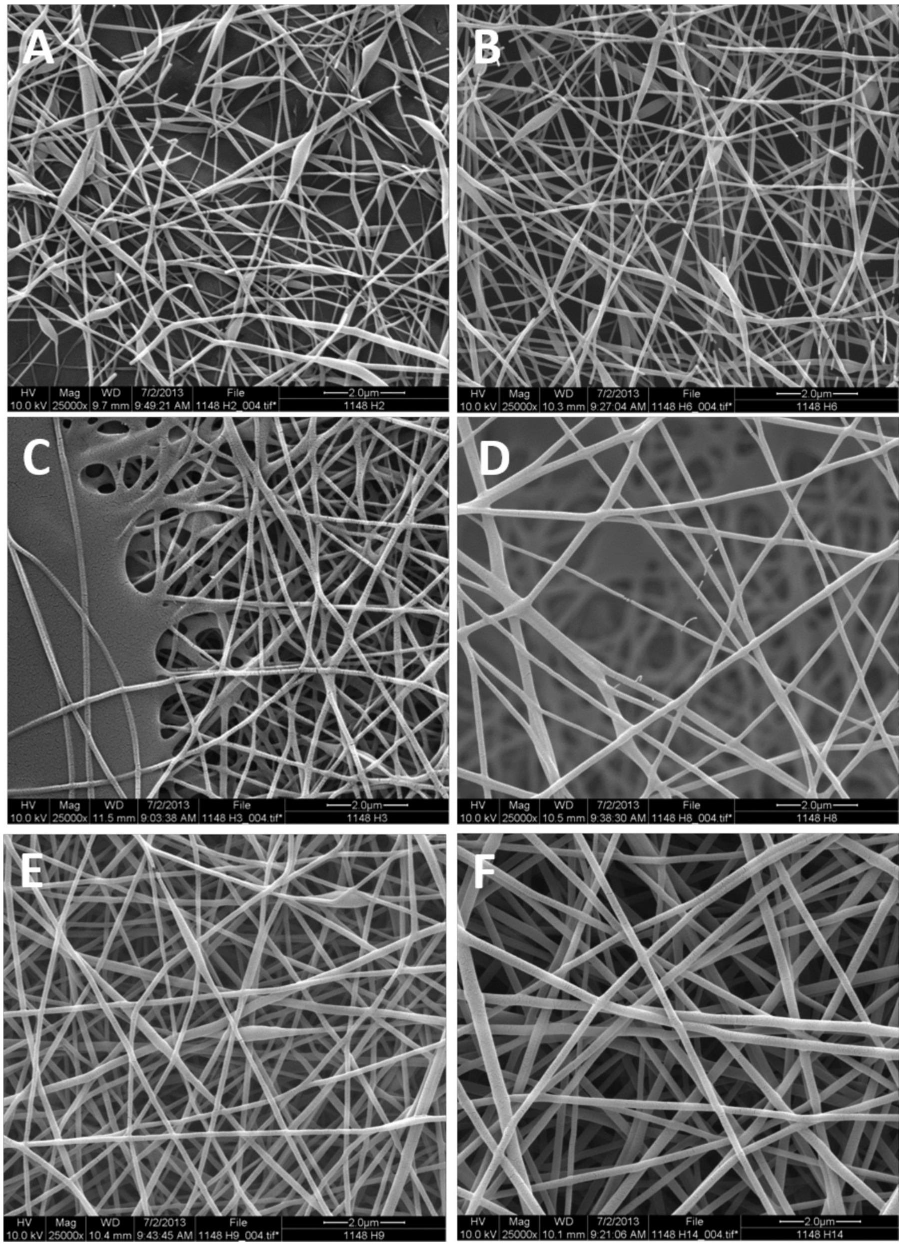

Fig. 6. Representative SEM pictures of the agar/PVA fibers produced by electrospinning and using water as solvent, at 25,000× magnification (agar 1 wt%/PVA 10 wt% ratios: (A) 50/50; (B) 40/60; (C) 30/70; (D) 20/80 obtained with E.4 conditions; (E) 20/80 obtained with E.5 conditions; (F) 0/100). Details concerning the process conditions are given in Table 1.

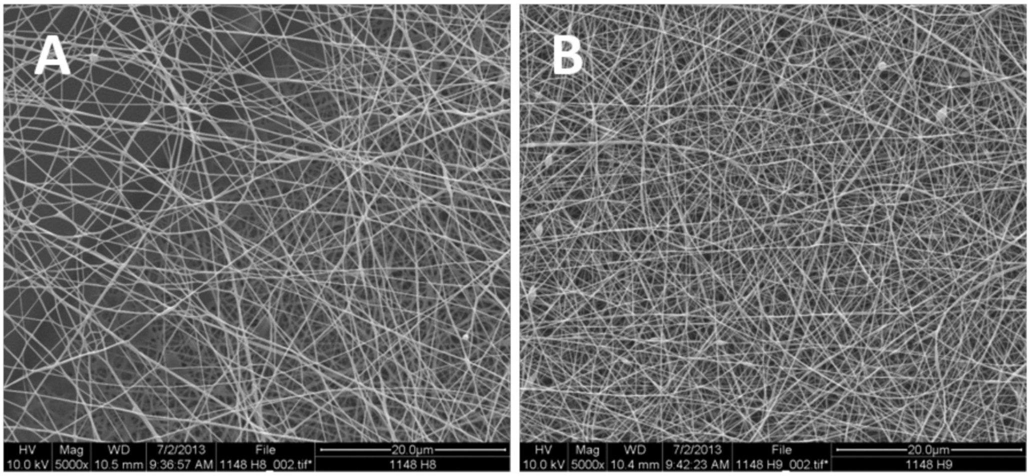

Fig. 7. SEM pictures of the 20/80 agar/PVA fibers displayed in Fig. 6D (obtained with E.4 conditions; A) and E (obtained with E.5 conditions; B) at lower magnification (5000×).

the needle. Constraints related to the temperature controller (*i.e.* variable temperature profile inside the chamber) could have contributed to agar gelation over the course of the experiments.

All together, these results indicate that high flow rates (14 mL/h) coupled with high voltages (24–30 kV), seemed more effective at producing agar/PVA nanofibers when using water as solvent. Discarding the processing difficulties, agar/PVA nanofibers were successfully spun particularly at higher PVA contents (70% or higher). The nature of the polymer jets seemed to indicate some incompatibility between both polymers in aqueous media, particularly at higher agar contents. However, this is a suggestion that needs to be confirmed. Currently, there are ongoing researches aiming at improving the temperature control inside the electrospinning chamber as well as exploring other components to improve the solutions spinnability.

4. Conclusions

Agar containing PVA nanofibers were successfully obtained by electrospinning technique using a tubeless spinneret attached inside the electrospinning chamber, with the temperature set at 50 °C. The PVA addition was crucial to improve the solutions spinnability as seen by the rheological profiles of the tested agar/PVA blends. Best nanofibers were obtained at higher PVA concentrations (*i.e.* 30/70 and 20/80 agar/PVA) while blends with higher agar contents (*i.e.* 40/60 and 50/50 agar/PVA) were harder to process. This first study can open a new window of opportunities for the fabrication of agar-based biomaterials in the form of nanofibers.

Acknowledgements

This work is funded by FEDER funds through the Operational Programme for Competitiveness Factors - COMPETE and by National Funds through FCT- Foundation for Science and Technology under the project Pest-C/EQB/LA0006/2013 – FCOMP-01-0124-FEDER-37285. FCT is also truly acknowledged for the concession of A.M.M. Sousa's PhD grant (SFRH/BD/64315/2009). To all financing sources the authors are greatly indebted.

References

Agarwal, S., Wendorff, J. H., & Greiner, A. (2008). Use of electrospinning technique for biomedical applications. *Polymer*, *49*, 5603–5621.

Bao, X. X., Hayashi, K., Li, Y. A., Teramoto, A., & Abe, K. (2010). Novel agarose and agar fibers: Fabrication and characterization. *Materials Letters*, *64*(22), 2435–2437.

Barber, P. S., Griggs, C. S., Bonner, J. R., & Rogers, R. D. (2013). Electrospinning of chitin nanofibers directly from an ionic liquid extract of shrimp shells. *Green Chemistry*, *15*(3), 601–607.

Bastos, D. S., Barreto, B. N., Souza, H. K. S., Bastos, M., Rocha-Leao, M. H. M., Andrade, C. T., et al. (2010). Characterization of a chitosan sample extracted from Brazilian shrimps and its application to obtain insoluble complexes with a commercial whey protein isolate. *Food Hydrocolloids*, *24*(8), 709–718.

Bonino, C. A., Krebs, M. D., Saquing, C. D., Jeong, S. I., Shearer, K. L., Alsberg, E., et al. (2011). Electrospinning alginate-based nanofibers: From blends to crosslinked low molecular weight alginate-only systems. *Carbohydrate Polymers*, *85*(1), 111–119.

Briscoe, B., Luckham, P., & Zhu, S. (2000). The effects of hydrogen bonding upon the viscosity of aqueous poly(vinyl alcohol) solutions. *Polymer*, *41*(10), 3851–3860.

de Moraes, M. A., & Beppu, M. M. (2013). Biocomposite membranes of sodium alginate and silk fibroin fibers for biomedical applications. *Journal of Applied Polymer Science*, *130*(5), 3451–3457.

Djabourov, M., Clark, A. H., Rowlands, D. W., & Ross-Murphy, S. B. (1989). Small angle X-ray scattering characterization of agarose sols and gels. *Macromolecules*, *22*(1), 180–188.

Gao, H.-W., Yang, R.-J., He, J.-Y., & Yang, L. (2010). Rheological behaviors of PVA/H_2O solutions of high-polymer concentration. *Journal of Applied Polymer Science*, *116*(3), 1459–1466.

Greiner, A., & Wendorff, J. H. (2007). Electrospinning: A fascinating method for the preparation of ultrathin fibres. *Angewandte Chemie International Edition*, *46*(30), 5670–5703.

Han, T., Yarin, A. L., & Reneker, D. H. (2008). Viscoelastic electrospun jets: Initial stresses and elongational rheometry. *Polymer*, *49*, 1651–1658.

Hassan, C. M., & Peppas, N. A. (2000). Structure and morphology of freeze/thawed PVA hydrogels. *Macromolecules*, *33*(7), 2472–2479.

Jayakumar, R., Menon, D., Manzoor, K., Nair, S. V., & Tamura, H. (2010). Biomedical applications of chitin and chitosan based nanomaterials – A short review. *Carbohydrate Polymers*, *82*(2), 227–232.

Khanarian, N. T., Haney, N. M., Burga, R. A., & Lu, H. H. (2012). A functional agarose-hydroxyapatite scaffold for osteochondral interface regeneration. *Biomaterials*, *33*(21), 5247–5258.

Koski, A., Yim, K., & Shivkumar, S. (2004). Effect of molecular weight on fibrous PVA produced by electrospinning. *Materials Letters*, *58*(3–4), 493–497.

Krishnan, R., Sundarrajan, S., & Ramakrishna, S. (2013). Green processing of nanofibers for regenerative medicine. *Macromolecular Materials and Engineering*, *298*(10), 1034–1058.

Lu, J.-W., Zhu, Y.-L., Guo, Z.-X., Hu, P., & Yu, J. (2006). Electrospinning of sodium alginate with poly(ethylene oxide). *Polymer*, *47*(23), 8026–8031.

Luo, C. J., Stoyanov, S. D., Stride, E., Pelan, E., & Edirisinghe, M. (2012). Electrospinning versus fibre production methods: From specifics to technological convergence. *Chemical Society Reviews*, *41*(13), 4708–4735.

Luo, Y., Wang, S. G., Shen, M. W., Qi, R. L., Fang, Y., Guo, R., et al. (2013). Carbon nanotube-incorporated multilayered cellulose acetate nanofibers for tissue engineering applications. *Carbohydrate Polymers*, *91*(1), 419–427.

Ma, G., Fang, D., Liu, Y., Zhu, X., & Nie, J. (2012). Electrospun sodium alginate/poly(ethylene oxide) core–shell nanofibers scaffolds potential for tissue engineering applications. *Carbohydrate Polymers*, *87*(1), 737–743.

Matsuhashi, T. (1990). Agar. In P. Harris (Ed.), *Food gels* (pp. 1–51). New York: Elsevier Science Publishers.

Nie, H. R., He, A. H., Zheng, J. F., Xu, S. S., Li, J. X., & Han, C. C. (2008). Effects of chain conformation and entanglement on the electrospinning of pure alginate. *Biomacromolecules*, *9*(5), 1362–1365.

Peresin, M. S., Habibi, Y., Zoppe, J. O., Pawlak, J. J., & Rojas, O. J. (2010). Nanofiber composites of polyvinyl alcohol and cellulose nanocrystals: Manufacture and characterization. *Biomacromolecules*, *11*, 674–681.

Rinaudo, M. (2008). Main properties and current applications of some polysaccharides as biomaterials. *Polymer International*, *57*(3), 397–430.

Rodrigues, M. T., Lee, S. J., Gomes, M. E., Reis, R. L., Atala, A., & Yoo, J. J. (2012). Bilayered constructs aimed at osteochondral strategies: The influence of medium supplements in the osteogenic and chondrogenic differentiation of amniotic fluid-derived stem cells. *Acta Biomaterialia*, *8*(7), 2795–2806.

Rošic, R., Pelipenko, J., Kocbek, P., Baumgartner, S., Bester-Rogac, M., & Kristl, J. (2012). The role of rheology of polymer solutions in predicting nanofiber formation by electrospinning. *European Polymer Journal*, *48*(8), 1374–1384.

Safi, S., Morshed, M., Ravandi, S. A. H., & Ghiaci, M. (2007). Study of electrospinning of sodium alginate, blended solutions of sodium alginate/poly(vinyl alcohol) and sodium alginate/poly(ethylene oxide). *Journal of Applied Polymer Science*, *104*(5), 3245–3255.

Santoro, M., Marchetti, P., Rossi, F., Perale, G., Castiglione, F., Mele, A., et al. (2011). Smart approach to evaluate drug diffusivity in injectable agar-carbomer hydrogels for drug delivery. *The Journal of Physical Chemistry B*, *115*(11), 2503–2510.

Santos, C., Silva, C. J., Buettel, Z., Guimaraes, R., Pereira, S. B., Tamagnini, P., et al. (2014). Preparation and characterization of polysaccharides/PVA blend nanofibrous membranes by electrospinning method. *Carbohydrate Polymers*, *99*, 584–592.

Schiffman, J. D., & Schauer, C. L. (2008). A review: Electrospinning of biopolymer nanofibers and their applications. *Polymer Reviews*, *48*(2), 317–352.

Sittikijyothin, W., Sampaio, P., & Gonçalves, M. P. (2010). Microstructure and rheology of beta-lactoglobulin-galactomannan aqueous mixtures. *Food Hydrocolloids*, *24*(8), 726–734.

Sousa, A. M. M., Borges, J., Silva, A. F., & Gonçalves, M. P. (2013). Influence of the extraction process on the rheological and structural properties of agars. *Carbohydrate Polymers*, *96*(1), 163–171.

Sousa, A. M. M., Borges, J., Silva, F., Ramos, A. M., Cabrita, E. J., & Gonçalves, M. P. (2013). Shaping the molecular assemblies of native and alkali-modified agars in dilute and concentrated aqueous media via microwave-assisted extraction. *Soft Matter*, *9*(11), 3131–3139.

Stijnman, A. C., Bodnar, I., & Tromp, R. H. (2011). Electrospinning of food-grade polysaccharides. *Food Hydrocolloids*, *25*(5), 1393–1398.

Toskas, G., Hund, R. D., Laourine, E., Cherif, C., Smyrniotopoulos, V., & Roussis, V. (2011). Nanofibers based on polysaccharides from the green seaweed *Ulva Rigida*. *Carbohydrate Polymers*, *84*(3), 1093–1102.

Yamada, Y., Hozumi, K., Aso, A., Hotta, A., Toma, K., Katagiri, F., et al. (2012). Laminin active peptide/agarose matrices as multifunctional biomaterials for tissue engineering. *Biomaterials*, *33*(16), 4118–4125.

Zadeh, M. M. A., Keyanpour-Rad, M., & Ebadzadeh, T. (2014). Effect of viscosity of polyvinyl alcohol solution on morphology of the electrospun mullite nanofibres. *Ceramics International*, *40*(4), 5461–5466.